

# Nonhomologous RNA Recombination in Tombusviruses: Generation and Evolution of Defective Interfering RNAs by Stepwise Deletions

K. ANDREW WHITE AND T. JACK MORRIS\*

*School of Biological Sciences, University of Nebraska-Lincoln, Lincoln, Nebraska 68588-0118*

Received 21 July 1993/Accepted 4 October 1993

**We used a protoplast system to study the mechanisms involved in the generation and evolution of defective interfering (DI) RNAs of tomato bushy stunt tombusvirus (TBSV). Synthetic transcripts corresponding to different naturally occurring TBSV DI RNAs, or to various artificially constructed TBSV defective RNAs, were analyzed. The relative levels of competitiveness of different DI RNAs were determined by coinoculating their corresponding transcripts into protoplasts along with helper genomic RNA transcripts and monitoring the level of DI RNA accumulation. Further studies were performed to assess the contribution of naked DI RNA stability and DI RNA encapsidation efficiency to the observed levels of competitiveness. In addition, the ability of various defective RNAs to evolve to alternative forms was tested by serially passaging protoplast infections initiated with transcripts corresponding to helper genomic RNA and a single type of defective RNA. These studies, and the analysis of the sequences of observed recombinants, indicate that (i) replication competence is a major factor dictating DI RNA competitiveness and is likely a primary determinant in DI RNA evolution, (ii) DI RNAs are capable of evolving to both smaller and larger forms, and the rates at which various transitions occur differ, (iii) DI RNA-DI RNA recombination and/or rearrangement is responsible for the formation of the evolved RNA molecules which were examined, and (iv) sequence complementarities between positive- and negative-sense strands in the regions of the junctions suggest that, in some cases, base pairing between an incomplete replicase-associated nascent strand and acceptor template may mediate selection of recombination sites. On the basis of our data, we propose a stepwise deletion model to describe the temporal order of events leading to the formation of tombusvirus DI RNAs.**

Defective interfering (DI) RNAs represent incomplete viral RNA genomes which are incapable of self-replication (reviewed in reference 33). Deletion of essential coding regions in DI RNA molecules makes them dependent upon the parental helper genome for provision of *trans*-acting factors required for replication and packaging. The presence of these molecules in viral infections often leads to decreased virus yields, presumably because of competition with the helper genome for a limited supply of *trans*-acting factors (13, 34). DI RNAs are commonly found associated with animal virus infections of cultured cells after serial passage of virus at a high multiplicity of infection (22, 34). Passing virus at a high multiplicity of infection is thought to favor double infection of cells (i.e., with both helper and DI RNAs), thereby promoting further amplification of newly generated or existing DI RNAs.

In contrast to animal viruses, DI RNAs appear to be less prevalent in RNA virus infections of plants. Tomato bushy stunt virus (TBSV), the type member of the tombusvirus group, was the first plant virus for which authentic DI RNAs were definitively identified (11). Tombusviruses represent a group of small, icosahedral plant viruses which contain a monopartite single-stranded messenger-sense RNA genome of approximately 4.7 kb. Since the original description of the TBSV DI RNAs, there have been additional reports of DI RNAs associated with other tombusviruses (3, 29), as well as with several other diverse groups of RNA plant viruses (20, 28, 32, 36). Plant virus DI RNAs have been shown to accumulate *de novo* following high-multiplicity serial passage of an infec-

tion initiated with a DI RNA-free inoculum (20), and tombusvirus DI RNAs appear *de novo* under analogous passage conditions (4, 17, 29). Interestingly, cucumber necrosis tombusvirus (CNV) DI RNAs can accumulate in an initially infected plant when it is inoculated with a mutant viral genome unable to express the p20 nonstructural viral protein (29). The presence of DI RNAs in tombusvirus infections results in attenuation of symptoms (3, 11, 29). Conversely, DI RNAs of both turnip crinkle carmovirus (20) and broad bean mottle virus (32) have been shown to increase the severity of symptoms.

Despite the apparent ubiquity of DI RNAs, little is known about the mechanism(s) by which these molecules are generated. The copy choice model for DI RNA formation suggests that template switching by the replicase during RNA synthesis is responsible for the generation of these recombinant molecules (5, 19, 27). In this model, the actively copying RNA replicase and incomplete nascent strand dissociate from an RNA template and reinitiate synthesis either on a new RNA template or at a different position on the original template. It has been suggested that secondary structure plays a role in the selection of the recombination sites (23), and it has been proposed that RNA heteroduplex formation between two RNA templates could mediate such recombination events (2). A number of conserved sequence motifs have been identified just 3' to junctions in turnip crinkle carmovirus DI RNAs and satellite RNAs which may mediate replicase reinitiation (5). In one of these motifs, maintenance of a specific secondary structure is required for recombination (6).

Little information is available on the structural attributes of DI RNAs which dictate their level of competitiveness. The maintenance of *cis* elements involved in replication and pack-

\* Corresponding author. Mailing address: School of Biological Sciences, 348 Manter Hall, University of Nebraska-Lincoln, Lincoln, NE 68588-0118. Phone: (402) 472-6676. Fax: (402) 472-2083.

aging represents two obvious components which could influence fitness. An additional, less obvious feature which has recently been shown to influence the accumulation of both plant and animal virus DI RNAs is maintenance (in the DI RNA) of a hybrid open reading frame (7, 14, 37). For these cases, it was postulated that translation of the DI RNA may either stabilize it or be coupled to its replication and/or packaging. The criteria defining DI RNA competitiveness, of course, will vary depending on the parental virus, the host, and the environmental conditions.

In the present study, we identified factors which influence the competitiveness of DI RNAs and showed that these molecules can evolve to both smaller and larger forms. Our results indicate that DI RNA-DI RNA recombination and/or rearrangement is responsible for the generation of the evolved DI RNA forms. The potential for base pairing at junction sites between positive- and negative-sense DI RNAs suggests that, in some cases, complementarity may direct the selection of recombination sites. On the basis of our data, we propose a model to describe the steps involved in the generation and evolution of DI RNAs in toombusviruses.

## MATERIALS AND METHODS

**Plasmid construction and in vitro transcription.** The construction of plasmids containing infectious cloned cDNAs of the viral genomes of TBSV (TBSV-100) and CNV (K2/M5) has been described previously (10, 30). K2/M5 was kindly provided by D. Rochon. HS-7 is an infectious clone of TBSV genomic RNA (gRNA) which does not express a functional viral coat protein (35) and was generously supplied by Herman Scholthof. The construction of plasmids DI-72 and DI-73, containing cloned cDNAs of naturally occurring DI RNAs, has already been described (16, 17). DI-82 and DI-83 were constructed by digestion of TBSV-100 with *Bst*XI (coordinate 1391) and *Sph*I (in vector, 3' to the viral sequence) and replacement of the excised viral fragment with the corresponding *Bst*XI and *Sph*I fragments from DI-72 and DI-73, respectively. DI-93 was constructed by digesting DI-73 with *Bst*XI (1391) and *Sal*I (4501) and replacing the excised viral fragment with *Bst*XI-*Bam*HI (2441) and *Bam*HI-*Sal*I fragments from TBSV-100. The authenticity of constructs DI-82, DI-83, and DI-93 was verified by restriction enzyme analysis and dideoxynucleotide sequencing of the regions forming the new junctions.

In vitro transcription was carried out on *Sma*I-digested TBSV-100, K2/M5, HS-7, or DI derivatives (see Fig. 1) with an Ampliscribe T7 RNA polymerase transcription kit (Epicentre Technologies). Reactions were terminated by addition of  $\text{NH}_4$  acetate to a final concentration of 2 M, followed by extraction with phenol-chloroform-isoamyl alcohol and precipitation of the products with ethanol. The products were subsequently resuspended in double-distilled  $\text{H}_2\text{O}$  to which a half volume of 7 M LiCl was added. The mixture was incubated on ice for 2 to 3 h, and the precipitate was collected by centrifugation, resuspended in double-distilled  $\text{H}_2\text{O}$ , and precipitated with ethanol in the presence of 2 M  $\text{NH}_4$  acetate. RNA transcripts synthesized in vitro were quantified spectrophotometrically, and the quality of the transcripts was monitored by agarose gel electrophoresis.

**Protoplast preparation and inoculation.** Protoplasts were prepared from cucumber (variety Straight 8) cotyledons by using a previously published protocol (13) with minor modifications. Cotyledons were excised prior to the emergence of true leaves, and the lower epidermis was removed with forceps. Following enzyme digestion, protoplasts were pelleted and

washed as previously described (13), except that the protoplasts were banded a second time onto a 20% sucrose cushion. Purified protoplasts were inoculated with viral RNA transcripts prepared in vitro as described previously (13) and were incubated in a growth chamber under fluorescent lighting at 22°C for 24 h.

**RNA analysis.** Total nucleic acid was harvested from protoplasts 24 h postinoculation (p.i.) by resuspension in 300  $\mu\text{l}$  of a buffer containing  $2\times$  STE (24) and 1% sodium dodecyl sulfate. Following two extractions with phenol-chloroform-isoamyl alcohol, 100  $\mu\text{l}$  of 8 M  $\text{NH}_4$  acetate was added to the aqueous phase and the mixture was precipitated with ethanol. Aliquots (1/10) of the total nucleic acid preparation were separated either in neutral 1.4% agarose gels or in 4.5% polyacrylamide gels containing 8 M urea. Viral RNAs were detected either by staining with ethidium bromide or by electrophoretic transfer to nylon (Nytran; Schleicher & Schuell), followed by Northern (RNA) blot analysis (24).  $^{32}\text{P}$ -labeled probes used for viral RNA detection on Northern blots were prepared with a random priming kit (Pharmacia).

cDNAs corresponding to different DI RNA species were prepared by first isolating the RNAs from 4.5% polyacrylamide gels containing 8 M urea by the crush-and-soak method (25), followed by amplification with a reverse transcription-PCR. The eluted RNA was mixed with approximately 100 pmol of oligonucleotide P9 (5' GGCGGCCCGCATGCCCGGGCTG CATTTCGCAATGTTCC), which contained, 5' to 3', a GC clamp of eight residues, *Sph*I and *Sma*I restriction sites, and sequence complementary to the 3' 23 nucleotides of both TBSV and CNV gRNAs. The mixture was heated at 90°C for 2 min and then set at ambient temperature for 5 min. Extension of the primer was carried out at 45°C for 50 min in a 30- $\mu\text{l}$  volume containing  $1\times$  reverse transcriptase buffer (Bethesda Research Laboratories); 10 mM dithiothreitol; dATP, dCTP, dGTP, and dTTP at 0.7 mM each; and 200 U of Superscript II reverse transcriptase (Bethesda Research Laboratories). The reaction was then diluted to a final volume of 100  $\mu\text{l}$  and included the following: 100 pmol of oligonucleotide P8 (5' GGCGTCTAGATAATACGACTCACTATAGGAAA TTCTCCAGGATTTCTC),  $1\times$  vent buffer (New England BioLabs), and 2 U of Vent DNA polymerase (Bethesda Research Laboratories). Oligonucleotide P8 contained, 5' to 3', a four-residue GC clamp, an *Xba*I restriction site, a T7 RNA polymerase promoter, and a sequence identical to the 5' 21 nucleotides of the TBSV and CNV gRNAs. PCR was carried out under the following conditions: one cycle of 5 min at 94°C, 1 min at 55°C, and 2 min at 72°C; 35 cycles of 1 min at 94°C, 1 min at 55°C, and 1 min at 72°C; and one cycle of 2 min at 94°C, 1 min at 55°C, and 2 min at 72°C. PCR products were then extracted with phenol-chloroform-isoamyl alcohol and precipitated with ethanol. The products were subsequently digested with *Xba*I and *Sph*I, gel purified (GeneClean; Bio 101), and ligated into *Xba*I-*Sph*I-digested pUC19. Clones were sequenced by the dideoxynucleotide chain termination method. Some of the DNA sequencing was performed by the Center of Biotechnology DNA Sequencing Facility (University of Nebraska-Lincoln).

**RNA half-life determinations.** Approximately  $10^6$  cucumber cotyledon protoplasts were inoculated with 20 pmol of a synthetic RNA transcript corresponding to either DI-72 or DI-73 as already described. The protoplasts were washed with 3 ml of 10% mannitol prior to addition of incubation buffer to remove untransfected RNA. Aliquots containing approximately  $1.5 \times 10^4$  cells were removed at 0, 1, 2, 4, 8, and 16 h p.i., and the total nucleic acid from these cells was isolated. A quarter of the recovered total nucleic acid was separated in a

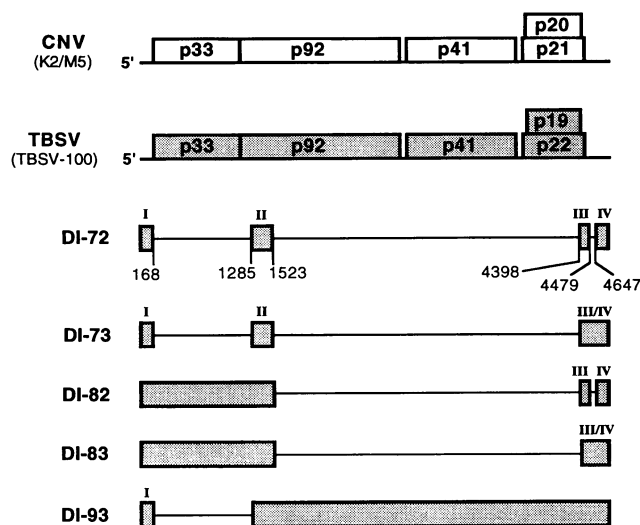


FIG. 1. Schematic representation of the gRNAs of CNV and TBSV and various naturally occurring DI RNAs (DI-72 and DI-73) and artificially constructed defective RNAs (DI-82, DI-83, and DI-93) of TBSV. The organization of the coding regions in the 4.7- and 4.8-kb gRNAs of CNV and TBSV, respectively, is shown at the top with the approximate  $M_r$ s of the encoded proteins (10, 31). Regions from which the TBSV DI RNAs were derived are shown below as shaded boxes, and the deleted intervening regions and depicted as lines. The coordinates given correspond to those of the gRNA of TBSV (10) and represent the junction sites for all of the DI RNAs shown. The four regions which are conserved, to some degree, in all of the characterized naturally occurring TBSV DI RNAs are indicated by roman numerals. Region III/IV represents a contiguous TBSV 3' terminus which includes the segment between regions III and IV.

neutral 1.3% agarose gel, electrophoretically transferred to nylon (Nytran), and hybridized with a  $^{32}\text{P}$ -labeled randomly primed probe corresponding to DI-73. Quantification of the bound RNA was performed by radioanalytic scanning of the membrane with the AMBIS Radioanalytic Imaging System (AMBIS Systems, Inc.).

## RESULTS

**Factors influencing competitiveness of DI RNAs.** We have shown previously that during high-multiplicity serial passage of TBSV in plants, a DI RNA species approximately 800 nucleotides (nt) long was the first dominant species to accumulate but, with continued passage, was replaced by a smaller, ~600-nt DI RNA species (16). The fact that the smaller species was the dominant DI RNA later in the passage series suggested that it was more competitive (i.e., more readily able to accumulate) than its larger counterpart. In the present study, we were interested in determining which of these DI RNA species is the more competitive and what factors influence the observed levels of competitiveness. cDNA copies corresponding to the larger (DI-73) and smaller (DI-72) DI RNA species had previously been cloned downstream of a T7 RNA polymerase promoter (16) and are shown schematically in Fig. 1. The nucleotide sequences of DI-73 and DI-72, which are 787 and 620 nt long, respectively, are identical, except that DI-72 contains a deletion of 167 nt in its 3' region (Fig. 1).

Transcripts of DI-73 and DI-72 prepared *in vitro* were tested for the ability to replicate and accumulate by coinoculation with a TBSV helper RNA transcript (TBSV-100; Fig. 1) into cucumber protoplasts. Total nucleic acid was prepared 24 h p.i.

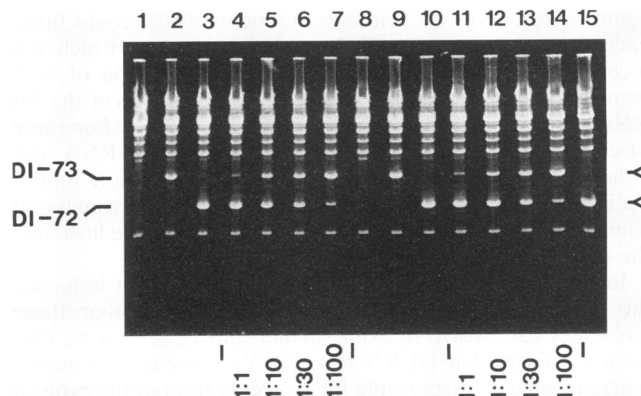


FIG. 2. Accumulation of DI-72 and DI-73 in cucumber protoplast infections with TBSV helper RNA transcripts. Approximately  $3 \times 10^5$  protoplasts were inoculated with various amounts of viral RNA transcripts prepared *in vitro*. Total nucleic acid was isolated 24 h p.i., and aliquots were separated in a 4.5% polyacrylamide gel in the presence of 8 M urea. The gel was stained with ethidium bromide. The helper RNA in the inoculations was either TBSV-100, which expresses coat protein, or HS-7, which does not. The inoculations were as follows: lane 1, TBSV-100 alone (2  $\mu\text{g}$ ); lane 2, TBSV-100 (2  $\mu\text{g}$ ) and DI-73 (0.34  $\mu\text{g}$ ); lane 3, TBSV-100 (2  $\mu\text{g}$ ) and DI-72 (0.27  $\mu\text{g}$ ); lane 4, TBSV-100 (2  $\mu\text{g}$ ), DI-72 (0.27  $\mu\text{g}$ ), and DI-73 (0.34  $\mu\text{g}$ ); lane 5, TBSV-100 (2  $\mu\text{g}$ ), DI-72 (0.27  $\mu\text{g}$ ), and DI-73 (3.4  $\mu\text{g}$ ); lane 6, TBSV-100 (2  $\mu\text{g}$ ), DI-72 (0.27  $\mu\text{g}$ ), and DI-73 (10.2  $\mu\text{g}$ ); lane 7, TBSV-100 (2  $\mu\text{g}$ ), DI-72 (0.27  $\mu\text{g}$ ), and DI-73 (34  $\mu\text{g}$ ). Inoculations in lanes 8 through 14 were as in lanes 1 through 7, except that the helper was HS-7 (2  $\mu\text{g}$ ). Lane 15 contained an infection with TBSV-100 (2  $\mu\text{g}$ ), DI-73 (0.27  $\mu\text{g}$ ), and torula yeast RNA (35  $\mu\text{g}$ ). The molar ratios of DI-72 to DI-73 in the inocula are indicated below lanes 4 to 7 and 11 to 14.

and analyzed by polyacrylamide gel electrophoresis under denaturing conditions. When TBSV-100 was coinoculated with either DI-73 or DI-72, RNA products corresponding to the sizes of these DI RNAs accumulated to levels readily detected by ethidium bromide staining (Fig. 2, lanes 2 and 3, respectively). No such RNA molecules accumulated when TBSV-100 alone was inoculated (Fig. 2, lane 1). When both DI-72 and DI-73 were coinoculated with TBSV-100 at a molar ratio of 1:1 (DI-72:DI-73), DI-72 accumulated to a level similar to that achieved when it was coinoculated with TBSV-100 alone (cf. lane 4 with lane 3 in Fig. 2). There was, however, a substantial reduction in the level of accumulation of DI-73 compared with when it was coinoculated with TBSV-100 alone (cf. lane 4 with lane 2 in Fig. 2). Further increases in the amount of DI-73 in coinoculations containing DI-72 and the helper (molar ratios of DI-72:DI-73, 1:10, 1:30, and 1:100) resulted in depression of DI-72 accumulation, concomitant with an increase in DI-73 accumulation (Fig. 2, lanes 5 to 7, respectively). Protoplasts inoculated with 34  $\mu\text{g}$  of the DI-73 transcript only (the mass used in the 1:100 coinoculations) showed no residual DI-73 remaining after the 24-h incubation (data not shown). To ensure that the observed reduction in the levels of DI-72 was the result of DI-73 in the inoculum, a coinoculation containing TBSV-100, DI-72, and 35  $\mu\text{g}$  of yeast RNA was performed (Fig. 2, lane 15). The accumulation of DI-72 to levels comparable to that achieved when DI-72 was coinoculated with the helper alone (cf. lane 15 with lane 3 in Fig. 2) indicated that the reduction in DI-72 levels in coinoculations with DI-73 was the result of active competition. These results demonstrate that DI-72 is more competitive than the larger DI-73.

There are several factors which could influence the compe-

tion observed between DI-72 and DI-73. The most obvious of these include the replication efficiency of the DI RNAs, the proficiency with which the DI RNAs are encapsidated, and the stability of the naked DI RNAs. To test the effect of encapsidation efficiency on the levels of accumulation of DI-72 and DI-73, a competition assay analogous to that performed with the wild-type TBSV-100 helper was carried out with a modified TBSV helper RNA transcript (HS-7; 35) which expresses a nonfunctional truncated coat protein (Fig. 2, lanes 8 to 14). With HS-7 as the helper, the accumulation profiles of DI-72 and DI-73 at the different inoculation ratios were indistinguishable from those in experiments with TBSV-100 as the helper (cf. lanes 11 to 14 with lanes 4 to 7 in Fig. 2). These results indicate that encapsidation does not significantly influence the relative levels of competitiveness of DI-72 and DI-73.

To assess the contribution of RNA stability to the observed levels of competitiveness, the half-lives of DI-72 and DI-73 were determined. Cucumber protoplasts were inoculated with equivalent moles of either DI-72 or DI-73 with no helper, and total nucleic acid was prepared from aliquots removed at various times after inoculation. The decay rate of each of the DI RNAs was determined following Northern blot analysis of the isolated total nucleic acid (Fig. 3A). The calculated half-lives of DI-72 and DI-73 were  $2.90 \pm 0.33$  and  $5.92 \pm 0.52$  h, respectively (Fig. 3B). In cucumber protoplasts, DI-73 was approximately twice as stable as DI-72. Therefore, the superior competitiveness of DI-72 cannot be attributed to the stability of its naked RNA. Taken together with the encapsidation data, this result implies that replication competence most likely represents a major contributing factor in the ability of DI-72 to accumulate to greater levels than DI-73 under competitive conditions. However, additional, undetermined factors may also have contributed to these results.

**Evolution of DI-73 to DI-72-like species.** We wanted to determine whether serial passage (in protoplasts) of an initial coinfection of DI-73 with the helper would allow evolution of DI-73 to a DI-72-like form. To ensure that the progeny DI RNAs examined represented derivatives of the input DI RNA, we used *in vitro*-synthesized RNA transcripts of a closely related tombusvirus, CNV, as the helper (30). CNV produces DI RNAs which are essentially identical in structure to those of TBSV (29) and can direct the replication of TBSV DI RNAs although the CNV and TBSV genomes differ at the nucleic acid level (64% identity; 10, 31). This sequence difference allowed (i) distinction between input TBSV DI RNAs and any DI RNAs produced *de novo* from the CNV helper RNA and (ii) identification of any helper-DI RNA recombinants. When K2/M5 (CNV; Fig. 1) was used as the helper, the relative accumulation levels of DI-72 and DI-73 were comparable to the levels observed when TBSV-100 was used as the helper (cf. lanes 1 to 7 in Fig. 4A with lanes 1 to 7 in Fig. 2).

DI-73 transcripts were coinoculated with K2/M5 into cucumber protoplasts, and the infection was subjected to 10 serial passages with total nucleic acid as the inoculum. Two different amounts of initial DI-73 inoculum were used, 0.34 (high) and 0.0034 (low)  $\mu\text{g}$ , and three sets of protoplasts were inoculated with each amount. The levels of accumulation of DI-73 in the initial coinfections at high and low DI-73 concentrations are shown in the left panel of Fig. 4B (lanes 1 to 3 and 4 to 6, respectively). No DI-73-sized RNAs accumulated in the initial infection when either K2/M5 alone or a mock inoculum was used (Fig. 4B, lanes 8 and 7, respectively). The initial infections (Fig. 4B, lanes 1 to 8) were then subjected to 10 serial passages, and total nucleic acid isolated from protoplasts of passage 10 were analyzed (Fig. 4B, lanes 9 to 16, respectively). All six infections which were initially coinoculated with DI-73 and

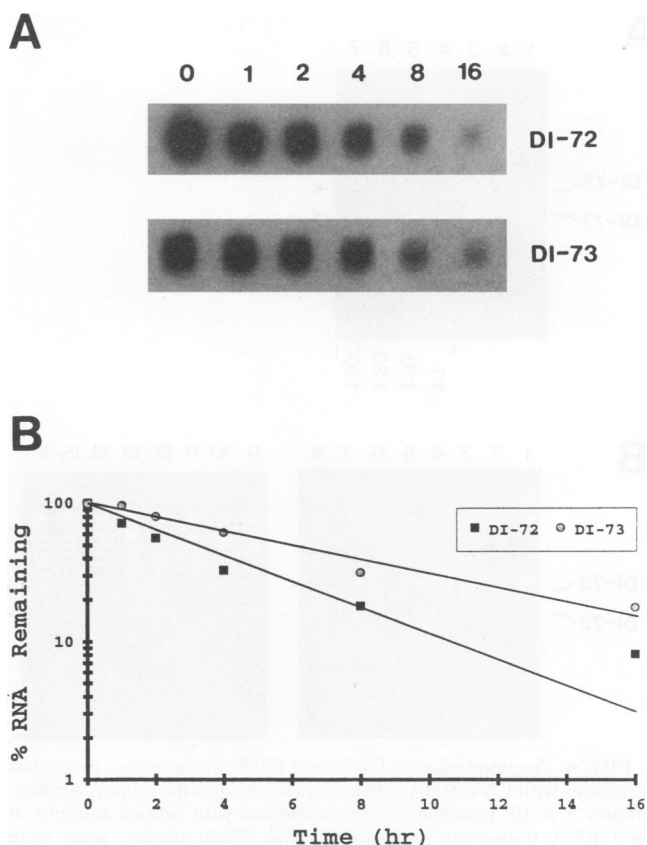


FIG. 3. Stability of DI-72 and DI-73 in cucumber protoplasts. DI RNA stability was determined following Northern blot analysis of total nucleic acid extracted from protoplasts inoculated with either DI-72 or DI-73 alone. (A) Aliquots of cells (approximately  $1.5 \times 10^5$ ) were removed at 0, 1, 2, 4, 8, and 16 h p.i., and the total nucleic acid was isolated. Aliquots of the total nucleic acid isolated were separated in a neutral 1.4% agarose gel, transferred to nylon, and hybridized with a  $^{32}\text{P}$ -labeled probe corresponding to DI-73. (B) The data shown in panel A were quantified by radioanalytic scanning of the membrane and are shown on a semilogarithmic plot. The decay rates were derived from the slopes of the lines as determined by linear regression analysis. The half-lives calculated from the data above were  $2.90 \pm 0.33$  h for DI-72 and  $5.92 \pm 0.52$  h for DI-73. In an independent set of inoculations, the calculated half-lives of DI-72 and DI-73 were  $3.00 \pm 0.34$  and  $5.86 \pm 0.92$  h, respectively (data not shown).

K2/M5 showed accumulation of DI-72-sized RNA species (Fig. 4B, lanes 9 to 14). DI-72-sized species were the primary accumulating products in infections with a high concentration of DI-73 (Fig. 4B, lanes 9 to 11). Infections with a low concentration of DI-73, however, showed a greater degree of variation, with accumulation of both DI-72-sized and intermediate-sized DI RNAs (Fig. 4B, lanes 12 to 14). The initial infection with K2/M5 alone after 10 passages showed accumulation of a DI-73-sized species (Fig. 4B, lane 16) which first appeared at passage 8. When cDNAs corresponding to this RNA species were cloned and sequenced, the sequences revealed that it represented a DI-73 contaminant rather than a DI RNA generated *de novo* from the CNV genome. This finding does not invalidate our findings regarding the DI-73-to-DI-72-like transition but instead illustrates the importance of using a helper RNA which is distinguishable from the DI RNA under study. Sequence analysis of cloned cDNAs corresponding to several of the DI-72-sized molecules which accu-

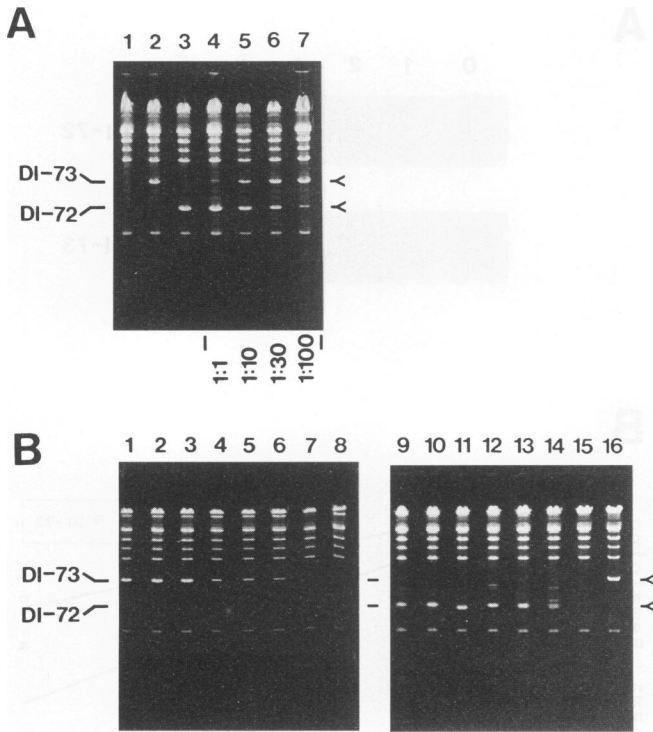


FIG. 4. Accumulation of DI-72 and DI-73 in cucumber protoplast infections with CNV RNA transcripts (K2/M5) as the helper. Approximately  $3 \times 10^5$  protoplasts were inoculated with various amounts of viral RNA transcripts prepared in vitro. Total nucleic acids were isolated 24 h p.i., and aliquots were separated in 4.5% polyacrylamide gels in the presence of 8 M urea. The gels were stained with ethidium bromide. (A) The inoculations were as follows: lane 1, K2/M5 alone (2  $\mu$ g); lane 2, K2/M5 (2  $\mu$ g) and DI-73 (0.34  $\mu$ g); lane 3, K2/M5 (2  $\mu$ g) and DI-72 (0.27  $\mu$ g); lane 4, K2/M5 (2  $\mu$ g), DI-72 (0.27  $\mu$ g), and DI-73 (0.34  $\mu$ g); lane 5, K2/M5 (2  $\mu$ g), DI-72 (0.27  $\mu$ g), and DI-73 (3.4  $\mu$ g); lane 6, K2/M5 (2  $\mu$ g), DI-72 (0.27  $\mu$ g), and DI-73 (10.2  $\mu$ g); lane 7, K2/M5 (2  $\mu$ g), DI-72 (0.27  $\mu$ g), and DI-73 (34  $\mu$ g). The molar ratios of DI-72 to DI-73 in the inocula for lanes 4 to 7 are shown below the lanes. (B) Transition of DI-73 to DI-72-sized products after 10 serial passages. The left panel (lanes 1 to 8) shows the separation of total nucleic acids isolated from protoplasts which were initially inoculated with viral transcripts. The inoculations were as follows: lanes 1 to 3, K2/M5 (2  $\mu$ g) and DI-73 (0.34  $\mu$ g); lanes 4 to 6, K2/M5 (2  $\mu$ g) and DI-73 (0.0034  $\mu$ g); lane 7, mock infection; lane 8, K2/M5 alone (2  $\mu$ g). Lanes 9 to 16 (right panel) represent total nucleic acids isolated from protoplasts from passage 10 following serial passage of the infections shown in lanes 1 to 8, respectively. Passages were carried out by inoculating a new set of protoplasts with one-fourth of the total nucleic acids isolated from the previous infection. The positions of DI-72 and DI-73 are indicated.

mulated in passages 7 and 9 confirmed their predicted DI-72-like structure and revealed a total of seven different junction types between regions III and IV (Fig. 5). The DI-72-like molecules contained no helper RNA sequences, thus confirming their derivation from DI-73. These results show that in our system, DI-73 is able to evolve to a DI-72-like species.

To observe the steps involved in the transition of DI-73 to the DI-72-like species, all of the products from a single passage series were separated in the same gel (Fig. 6). The accumulated products from the initial infection with K2/M5 and DI-73 (lane 0) through passages 1 to 10 (lanes 1 to 10, respectively) are shown in Fig. 6. During the passaging, there was decreased accumulation of DI-73 concomitant with increased accumula-

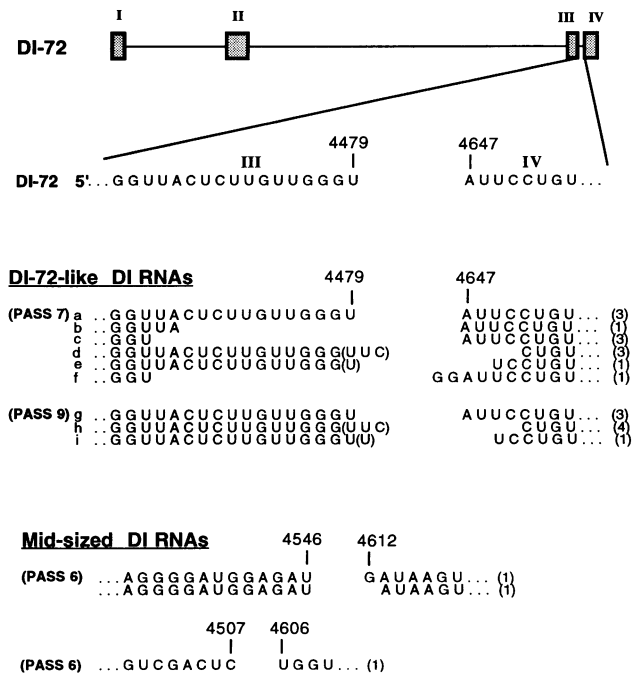


FIG. 5. Sequences at the junction between regions III and IV in DI-72-like and mid-sized DI RNAs which were generated from DI-73 during serial passage with the helper. A schematic representation of DI-72 is shown at the top with the corresponding sequences flanking regions III and IV. Below are the sequences flanking the junction of regions III and IV for DI-72-like molecules from passages 7 and 9 and for mid-sized DI-RNAs isolated from passage 6. The sequences shown for DI-72-like and mid-sized DI RNAs were determined from cloned cDNAs corresponding to DI RNAs isolated from passages originating from four or two different initial inoculations, respectively. The numbers in parentheses at the right represent the total numbers of clones which contained the sequences. The nucleotides in parentheses were arbitrarily placed with the upstream junction.

tion of a prominent DI-72-sized product (Fig. 6). The profile of the accumulated products is representative of passages from initial inoculations with high concentrations of DI-73. For passages initiated with the low concentration of DI-73, the transition was delayed by approximately 1 to 2 passages (data not shown). A Northern blot of the stained gel revealed the presence of a less abundant DI RNA species which was intermediate in size between DI-73 and the DI-72-like product (Fig. 6, lower panel). These mid-sized DI RNAs (designated M in Fig. 6) were clearly detectable approximately 1 passage after the DI-72-like product began to accumulate (cf. lane 3 with lane 2 in the lower panel of Fig. 6). The kinetics of accumulation therefore suggest that the mid-sized DI RNAs do not necessarily represent intermediates in the DI-73-to-DI-72-like product conversion. Sequence analysis of cloned cDNAs corresponding to a number of DI-73-derived mid-sized molecules demonstrated that they contained various small ( $\leq 98$ -nt) deletions of the segment between regions III and IV (Fig. 5).

In one of the passage series of DI-73 with K2/M5, a larger DI RNA (designated DI-R1) was detected and became the dominant DI RNA species at passage 6 (Fig. 7A, lane 3) but was no longer detectable at passage 10 (Fig. 4B, lane 12). No DI RNA species were detected in the corresponding sixth passage of inoculations with K2/M5 alone or the mock inoculation (Fig. 7A, lanes 2 and 1, respectively). Cloning and sequencing of several cDNAs corresponding to DI-R1 re-

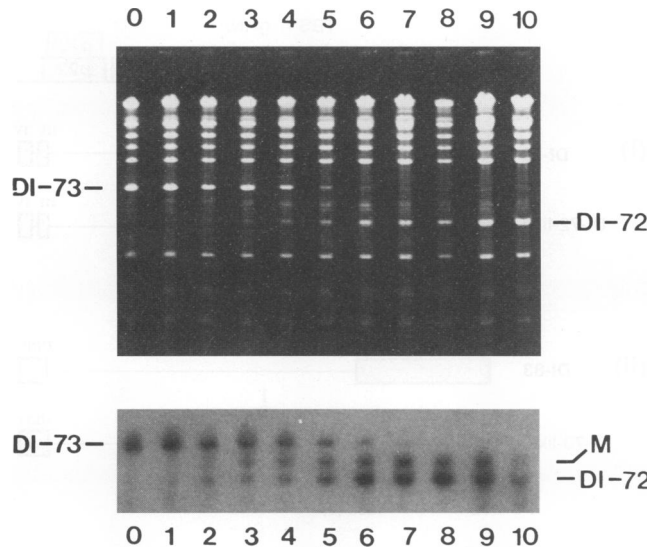


FIG. 6. Transition of DI-73 to a DI-72-like product during 10 serial passages in cucumber protoplasts. Aliquots of total nucleic acids isolated 24 h p.i. from the initial infection (lane 0) and from 10 serial passages (lanes 1 to 10, respectively) were separated in a 4.5% polyacrylamide gel in the presence of 8 M urea and stained with ethidium bromide (upper panel). The nucleic acids in this gel were subsequently transferred to nylon and hybridized with a <sup>32</sup>P-labeled probe corresponding to DI-73 (lower panel). The positions of DI-72, DI-73, and the intermediate-sized DI RNA (M) are indicated.

vealed that it retained regions I and III/IV of DI-73 but contained a duplication of a 130-nt segment in region II which accounted for its larger size (Fig. 7B). The duplication of a DI RNA-specific region and the absence of any helper sequence indicated either a recombination event between DI RNAs or rearrangement.

**Accumulation and evolution of putative DI RNA precursors.**

Previous studies on tombusvirus DI RNA formation and evolution were unable to detect any molecules larger than DI-73 (4, 16, 17, 29). Presumably, larger precursors do exist but, for unknown reasons, cannot accumulate to detectable levels or are transient. To explore the possible existence of larger DI RNA precursors, we synthesized *in vitro* large artificial defective RNAs (DI-82, DI-83, and DI-93; Fig. 1) from plasmid constructs containing their corresponding cloned cDNAs. The segment between regions I and II, which is deleted in DI-72 and DI-73, was reintroduced to produce DI-82 and DI-83, respectively (Fig. 1). Similarly, the segment between regions II and III/IV, which is deleted in DI-73, was reintroduced to produce DI-93 (Fig. 1). Transcripts corresponding to these putative DI RNA precursors were individually inoculated with K2/M5 into cucumber protoplasts, and the total nucleic acid was isolated 24 h p.i. and analyzed by Northern blotting (Fig. 8A). Mock inoculation or inoculation of DI-82, DI-83, or DI-93 alone resulted in no detectable accumulation of viral RNA (Fig. 8A, lanes 1, 6, 7, and 8, respectively). Inoculation with K2/M5 alone resulted in accumulation of helper gRNA and the two subgenomic RNAs (Fig. 8A, lane 2). RNA products corresponding to the predicted sizes of DI-82 (~1.7 kb) and DI-83 (~1.9 kb) were readily detectable when DI-82 or DI-83 was coinoculated with the helper (Fig. 8A, lanes 3 and 4, respectively). Stained gels revealed that these two defective RNAs did not accumulate to high levels (data not shown). Their apparent high level of

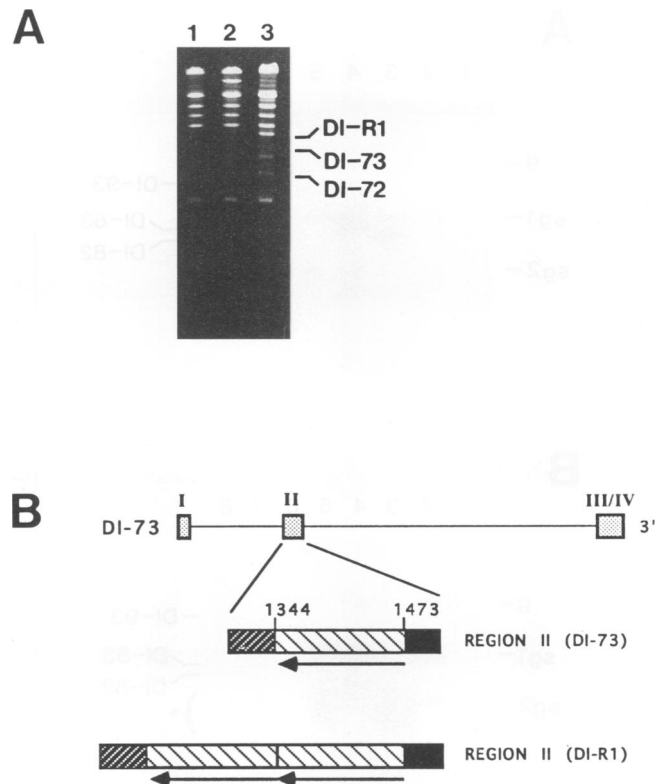


FIG. 7. Accumulation of DI-R1 in passage 6 from an initial inoculation with DI-73 and K2/M5. (A) Total nucleic acids were isolated from protoplasts of passage 6 and separated in a 4.5% polyacrylamide gel in the presence of 8 M urea. The gel was stained with ethidium bromide. The initial inoculations were as follows: lane 1, mock infection; lane 2, K2/M5 alone; lane 3, K2/M5 and DI-73. The positions of DI-73, DI-72, and DI-R1 are indicated. (B) Schematic representation of the structures of DI-73 and DI-R1. The complete structure of DI-73 is shown with an enlargement of region II. DI-R1 contains regions I and III/IV of DI-73 but, as shown, contains a direct duplication of a segment in region II (arrows). The coordinates indicated for the duplicated region correspond to those of the gRNA of TBSV (10).

accumulation was the result of hybridization of the blot with a TBSV-specific probe which was entirely complementary to DI-82 and DI-83 but was only partially complementary to the CNV RNAs. No RNA with the predicted size of DI-93 (~3.7 kb) was detected when it was coinoculated with the helper (Fig. 8A, lane 5).

The initial infections shown in Fig. 8A (lanes 1 to 8) were then subjected to a single passage, and the total nucleic acid from these protoplasts was examined by Northern blotting (Fig. 8B, lanes 1 to 8, respectively). No viral RNAs were detected in protoplasts passaged from either the mock inoculation or inoculation of DI-82, DI-83, or DI-93 alone (Fig. 8B, lanes 1, 6, 7, and 8, respectively), but authentic viral RNAs were detected upon passage of the helper alone (Fig. 8B, lane 2). When coinfections of the helper with either DI-82 or DI-83 were passaged, DI-82- and DI-83-sized progeny accumulated (Fig. 8B, lane 3 and 4, respectively) along with RNAs similar in size to DI-72–DI-73 molecules (Fig. 8B, asterisk). Passage of the infection with DI-93 and the helper also resulted in accumulation of similar small viral RNA products (Fig. 8B, lane 5), even though there was no detectable accumulation of

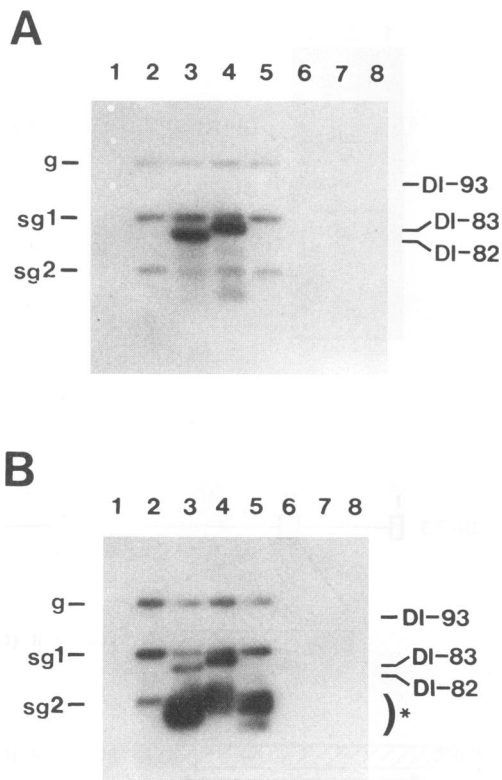


FIG. 8. Accumulation and evolution of putative precursor DI RNAs (DI-82, DI-83, and DI-93) in cucumber protoplast infections. Northern blots of total nucleic acids isolated 24 h p.i. from the initial protoplast infection (A) or from a single passage of the initial infection (B) were hybridized with a  $^{32}\text{P}$ -labeled probe corresponding to the 3' terminus of TBSV gRNA. Samples were separated in neutral 1.4% agarose gels. (A) The inoculations were as follows: lane 1, mock infection; lane 2, K2/M5 alone (2  $\mu\text{g}$ ); lane 3, K2/M5 (2  $\mu\text{g}$ ) and DI-82 (2  $\mu\text{g}$ ); lane 4, K2/M5 (2  $\mu\text{g}$ ) and DI-83 (2  $\mu\text{g}$ ); lane 5, K2/M5 (2  $\mu\text{g}$ ) and DI-93 (3  $\mu\text{g}$ ); lane 6, DI-82 alone (2  $\mu\text{g}$ ); lane 7, DI-83 alone (2  $\mu\text{g}$ ); lane 8, DI-93 alone (3  $\mu\text{g}$ ). (B) Accumulated products after a single passage of the infections in lanes 1 to 8 of panel A. The passage was carried out by inoculating a new set of protoplasts with one-fourth of the total nucleic acids isolated from the initial infection. The positions of the CNV gRNA (g [4.7 kb]) and subgenomic RNAs (sg1 [2.1 kb] and sg2 [0.9 kb]) are shown to the left. The positions of DI-82 and DI-83 and the anticipated position of DI-93 are shown to the right. The position of newly generated small RNAs is indicated by the asterisk.

DI-93-sized progeny in either the original infection or the subsequent passage. In other experiments, however, we showed that DI-93 is able to replicate and accumulate to low but detectable levels in initial infections when it is coinoculated at high concentrations with the helper (data not shown). It is likely, therefore, that there was a "subliminal" level of replication of DI-93 in the experiment whose results are shown in Fig. 8, the accumulation of which was below the detection level of our assay. This result provides evidence that small DI RNA-like molecules can be rapidly generated from a larger precursor which does not accumulate to detectable levels. The accumulation of small DI-72- and DI-73-sized products from DI-93, DI-83, and DI-82 within a single passage was reproducible in several additional experiments with independently prepared transcripts and protoplasts. We cloned and se-

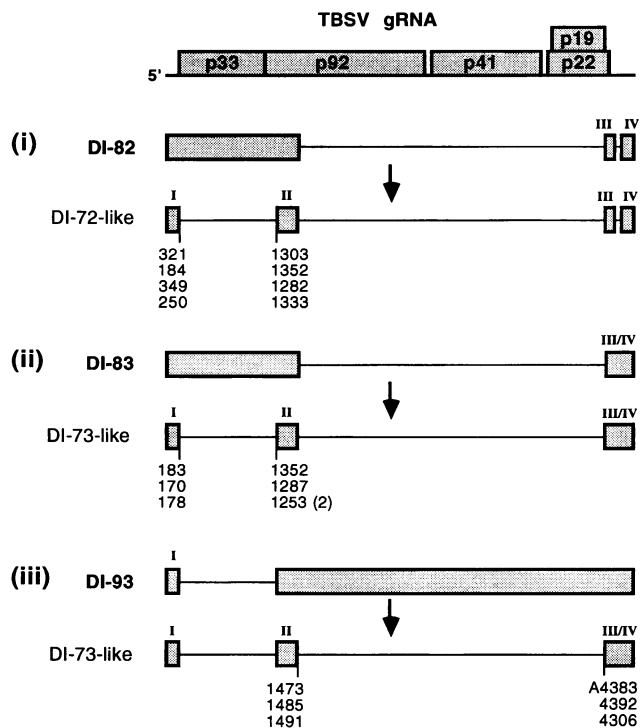


FIG. 9. Schematic representation of the transitions of large putative DI RNA precursors to smaller DI RNA species after a single passage. The gRNA of TBSV is shown schematically at the top, and the transitions observed for DI-82, DI-83, and DI-93 are shown below. The coordinates given correspond to those of the gRNA of TBSV (10). The number in parentheses in diagram ii indicates that two independent clones contained that junction. The letter A in front of the coordinate in diagram iii represents an inserted adenosine residue at that junction.

quenced several cDNAs corresponding to the smaller DI RNA-like molecules generated, and the structures of these molecules are shown schematically in Fig. 9. The sequences revealed that the segment between regions I and II was deleted to various degrees in DI-82 and DI-83 to generate DI RNAs with DI-72- and DI-73-like structures (Fig. 9, i and ii), respectively, and that DI-73-like molecules were generated from DI-93 by various deletions between regions II and III/IV (Fig. 9, iii). The presence of unique junctions and of additional viral sequences not present in either DI-72 or DI-73 in the newly formed DI RNAs eliminated the possibility that they arose through contamination (Fig. 9). In addition, the DI-72/73-like molecules generated contained no helper genome sequences. These results demonstrate that the larger defective RNAs can serve as precursors for the more prototypical DI RNA forms.

## DISCUSSION

RNA recombination among viruses containing RNA genomes is now an accepted phenomenon. This process is becoming increasingly recognized as an important mechanism in RNA virus evolution and genome repair and, in some cases, may play a crucial role in normal genome replication (18). The facility with which tombusviruses generate DI RNAs makes them ideal subjects for studying facets of RNA recombination and evolution. To this end, we used a protoplast system to (i) analyze factors which influence the competitiveness of these

molecules and (ii) investigate possible mechanisms for TBSV DI RNA generation and evolution.

**DI RNA competitiveness.** Our results suggest that replication ability likely represents a major factor influencing DI RNA accumulation levels under competitive conditions. It seems unlikely that the difference in size between the two DI RNAs (620 versus 787 nt) could, on its own, account for the disparity in replication efficiency. It is possible that deletion of the 167-nt segment made DI-72 more proficient at recruiting and/or utilizing *trans*-acting replication elements, thus making it more competitive. The finding that DI-72 is more competitive than DI-73 is relevant in light of the fact that when protoplast infections initiated with DI-73 and the helper were serially passaged, the predominant accumulating DI RNAs had structures analogous to that of DI-72. It is likely that the same competitive properties of DI-72 and DI-73 which were defined experimentally are responsible for dictating the accumulation of the DI-72-like molecules generated from DI-73. Our results, therefore, suggest that for at least one of the steps in DI evolution (the DI-73-like to DI-72-like product conversion) replication efficiency is likely a major factor influencing the transition.

**Evolution of DI RNAs.** On the basis of our findings that DI-72-like molecules are derived from DI-73 during serial passage, we propose that *de novo* generation of DI-72-like molecules from the viral genome occurs by a similar mechanism (i.e., through a transient DI-73-like intermediate). Two possible modes by which the DI-73 to DI-72-like product transition could occur include (i) excision of the segment spanning regions III and IV by a series of progressively larger deletions (this scheme would involve intermediates) and (ii) a single deletion event leading to formation of DI-72-like molecules, each with different amounts of the 3' segment deleted. In the latter case, derivatives which resemble DI-72 (with approximately 167 nt deleted between regions III and IV) would presumably compete successfully against those with smaller deletions of this region. Our kinetic data on the DI-73 to DI-72-like product transition showed that the DI-72-like products began to accumulate prior to the mid-sized DI RNAs, suggesting that this transition may occur through an intermediate-independent (i.e., mid-sized DI RNA-independent) pathway.

We have demonstrated that larger putative DI RNA precursors accumulate to relatively low levels and rapidly transform to smaller DI-72- and DI-73-like molecules after a single passage. This result proves that these larger molecules could represent functional intermediates in the formation of smaller DI RNAs. Furthermore, the relatively low level of accumulation of the large precursor molecules and their capacity to evolve rapidly to DI-72- and DI-73-like molecules are features which are consistent with the lack of detection of comparable larger DI RNA precursors in previous studies.

We have characterized an atypical DI RNA, DI-R1, containing a duplication of a segment in region II. The identification of this DI RNA species, which accumulated to relatively high levels during passage of DI-73 with a helper, is significant in several respects. The finding that DI-R1 accumulated in passages 6 to 8 but was undetectable in earlier or later passages illustrates that (i) DI RNA populations are dynamic, (ii) timing is an important factor in identifying different DI RNA species, and (iii) duplication of this region must have conferred some selective advantage to DI-R1 during passages 6 through 8. Additionally, the result indicates that in some instances DI RNAs may recombine and/or rearrange to form larger DI RNAs, thus illustrating the ability to evolve to both smaller and larger molecules.

**Templates participating in RNA recombination and selection of recombination sites.** Sequence analysis of DI-72- and DI-73-like molecules generated from either DI-73 or larger precursors indicated that their formation did not involve recombination with the helper genome. This is in contrast to animal coronavirus DI RNAs, which are able to evolve via recombination with the helper genome (9). The generation of the TBSV DI RNAs must have, therefore, involved either inter- or intramolecular DI RNA recombination. Further attempts to determine which of these mechanisms functions in these conversions are under way.

The DI-73 to DI-72-like product transition was found to be facilitated by a higher concentration of DI-73 in the initial inoculation. In studies on poliovirus RNA recombination, it was determined that the greater the concentration of viral RNA, the higher the observed recombination frequency (12). Similarly, our results suggest that the concentration of a DI RNA population is an important factor in determining recombination frequency and, in turn, the facility with which DI RNA evolution occurs. In the case of intramolecular DI RNA recombination (i.e., rearrangement), the generation of recombinants would be predicted to increase linearly with the template concentration, whereas with intermolecular DI RNA recombination a faster increase would be expected because of the elevating probability for *trans* interactions as the template concentration increases.

To gain further insight into the mechanism(s) responsible for these recombination events, the sequences surrounding the junctions in newly generated DI RNAs were examined (Fig. 10A). Analysis of the upstream and downstream recombination sites for the deletions between regions III and IV indicated the potential for base pairing between positive- and negative-sense DI RNA strands, respectively (Fig. 10B to D). The 5' and 3' junction sites (upper and lower arrows, respectively) were found either directly across from or within a few residues of each other and were present either within or directly adjacent to base-paired tracts. This finding implies that regions which contain short stretches of complementarity represent preferred recombination sites. The tracts of complementarity to the left of the junctions in Fig. 10B and to the right of the junction in Fig. 10D suggest that these sequences could act as guides for repriming in a copy choice type of event during positive- or negative-sense strand synthesis, respectively. A schematic representation of such a recombination event between two DI RNAs in which template switching occurs during negative-sense strand synthesis is depicted in Fig. 10E. Similar mechanisms involving repriming by the 3' end of the incomplete nascent strand have been proposed for poliovirus (15), flock house virus (21), coronavirus (18), and Q $\beta$  phage (1). Examination of other newly generated junction sites (i.e., junctions I-II and II-III) in the DI-72- and DI-73-like molecules generated from the precursors showed various degrees of complementarity (data not shown), indicating that although the ability to base pair at junction sites may facilitate some recombination events, it is not a prerequisite. We also found that as in brome mosaic virus (2), stable heteroduplexes between same-sense strands can form between the sequences at some of the junction sites (data not shown). It is possible that several distinct mechanisms may function in tombusvirus RNA recombination to generate the variety of junctions that have been observed. Caution should be exercised when interpreting data concerning junction sites. It is essential that the effect of selective pressures on the accumulation of the recombinant be considered (26). For instance, a recombinant which is generated by an infrequent event may be preferentially amplified because of its highly competitive nature; however,



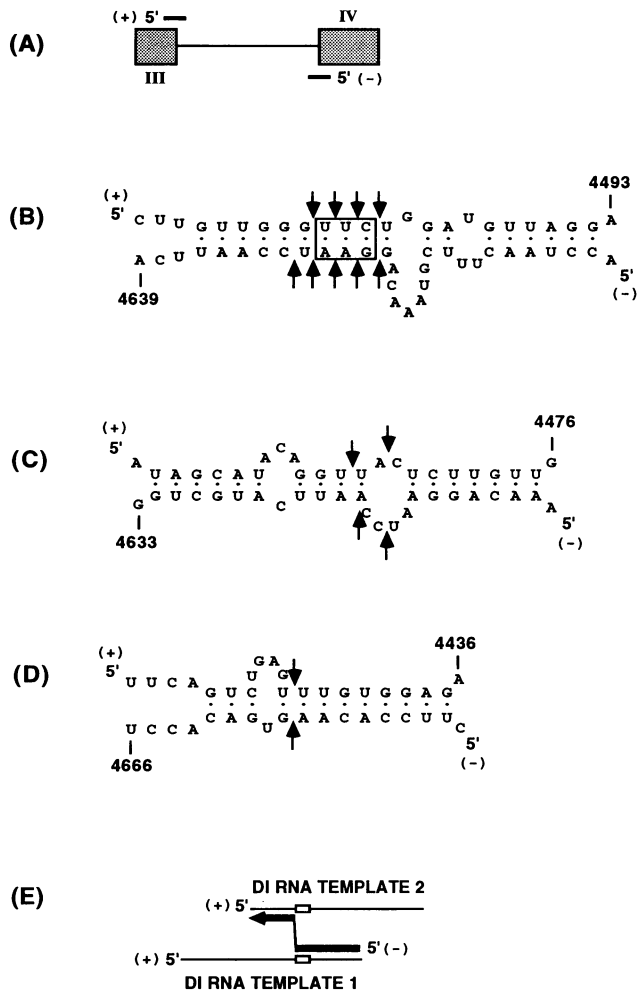


FIG. 10. Potential for base pairing between the positive-sense DI RNA strand sequence at the upstream recombination site and the negative-sense DI RNA strand sequence at the downstream recombination site for the junction between regions III and IV. (A) Schematic representation of regions III and IV (boxes) and the intervening sequence (thin line). The bold lines indicate the sequences (from both the DI RNA and the contiguous intervening regions) at the upstream and downstream junction sites which were examined for base-pairing potential. (B) Compilation of junctions a, d, e, g, h, and i from Fig. 5. The boxed residues could have been contributed by either upstream or downstream recombination sites. Upstream and downstream junction sites are indicated, respectively, by arrows above and below the sequences. (C) Compilation of junctions b, c, and f from Fig. 5. (D) Junction between regions III and IV observed in DI-72-like molecules in additional independent experiments (data not shown). The structures shown were generated with the FOLD program (8). To facilitate the analysis (which requires a single RNA molecule), the 3' ends of the positive-sense strands were joined to the 5' ends of the negative-sense strands by poly(A) tracts of four residues. (E) Example of a copy choice type of recombination event during negative-sense strand synthesis involving two positive-sense DI RNA templates. The bold line and arrow indicate the nascent negative-sense strand and the direction of elongation, respectively. Open boxes in the templates represent identical or similar sequence tracts located at two different positions in the two DI RNAs which could serve as guides for template switching. Following dissociation from template 1, the sequence at the 3' terminus of the incomplete nascent negative-sense strand (the complement of the sequence represented by a box in template 1) could reprime on template 2 by base pairing with a complementary sequence

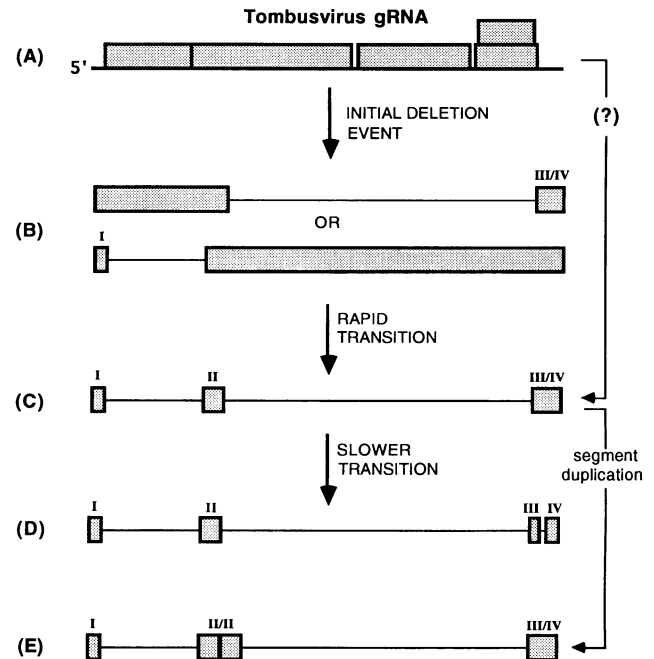


FIG. 11. Stepwise deletion model for generation and evolution of tombusvirus DI RNAs. Panels: A, viral gRNA; B, large DI RNA precursors; C, DI-73-like molecules; D, DI-72-like molecules; E, DI RNA containing a duplicated segment. See the Discussion for details.

the observed junction will not represent a recombination hot spot.

**Model to describe the temporal order of recombination events leading to formation of prototypical tombusvirus DI RNAs.** Not all recombinant viral RNAs which are initially generated will contain the necessary elements required for their amplification. There will be selective pressure on a newly generated recombinant to maintain certain sequences which will allow its amplification. In addition, the RNA molecule may evolve, via recombination and/or rearrangement, to a size which is compatible with its maximal competitiveness. On the basis of our data, we propose a stepwise deletion model to describe the stages involved in the generation and evolution of DI RNAs in tombusviruses (Fig. 11). Our results suggest that formation of the highly competitive DI-72-like species does not occur as a single event but instead is the consequence of stepwise deletions of segments in the gRNA. In our system, the formation of smaller DI RNA species involves DI RNA-DI RNA recombination and/or rearrangement, and accumulation of these molecules appears to be dictated primarily by replication efficiency. In the model, the initial deletion event in the gRNA (Fig. 11A) would involve the removal of either of the relatively large segments between regions I and II or regions II and III/IV (Fig. 11B). The removal of these segments could occur either (i) as a single deletion event or (ii) by accumulation of a series of smaller deletions. The products of the initial deletion event (Fig. 11B) do not accumulate to levels which are easily detectable but are substrates for subsequent deletion events, the products of which rapidly accumulate as DI-73-like

(open box in template 2). This model predicts a single copy of the guide sequence (which may be a hybrid) in the newly generated negative-sense strand.

species (Fig. 11C). Alternatively, we cannot discount the possibility that the DI-73-like species could be formed by concomitant removal of the two large segments. The DI-73-like molecules then make the slower transition to DI-72-like forms (Fig. 11D) through deletion of a 3' segment between regions III and IV. Rapid transition and slow transition are used as relative terms to describe the timing of accumulation of particular products. The rates of such transitions will be dependent upon (i) the frequency of the recombination events, (ii) the competitiveness of the recombinants generated, and (iii) the competitiveness of the precursors (and of other viral RNAs present). The latter factor may, in part, account for the rapid accumulation of DI-73-like molecules from the poorly accumulating large precursors and the slower accumulation of DI-72-like molecules from the more competitive DI-73 precursor. In some cases, DI-73-like molecules (and possibly other DI RNA species) may also recombine and/or rearrange to generate larger, presumably more competitive DI RNA species (Fig. 11E), thus illustrating an added degree of flexibility in DI RNA evolution. Attempts to investigate in further detail the mechanism(s) of RNA recombination in tombusviruses are under way. We anticipate that some of the features of the stepwise deletion model will be useful in the development of models for DI RNA generation and evolution in other viruses.

#### ACKNOWLEDGMENTS

We thank Andy Jackson, Herman Scholthof, Marc Law, Jim Skuzeski, and Laurie Baggio for critically reviewing the manuscript.

This research was supported by a grant from the Department of Energy (DE-FG03-88ER13908). K.A.W. was supported by a postdoctoral fellowship from the Natural Science and Engineering Research Council of Canada.

#### REFERENCES

- Biebricher, K. C., and R. Luce. 1992. In vitro recombination and terminal elongation of RNA by Q $\beta$  replicase. *EMBO J.* **11**:5129–5135.
- Bujarski, J. J., and A. M. Dzanott. 1991. Generation and analysis of nonhomologous RNA-RNA recombinant in brome mosaic virus: sequence complementarities at crossover sites. *J. Virol.* **65**:4153–4159.
- Burgyan, J., F. Grieco, and M. Russo. 1989. A defective interfering RNA molecule in cymbidium ringspot virus infections. *J. Gen. Virol.* **70**:235–239.
- Burgyan, J., L. Rubino, and M. Russo. 1991. De novo generation of cymbidium ringspot virus defective interfering RNA. *J. Gen. Virol.* **72**:505–509.
- Cascone, P. J., C. D. Carpenter, X. H. Li, and A. E. Simon. 1990. Recombination between satellite RNAs of turnip crinkle virus. *EMBO J.* **9**:1709–1715.
- Cascone, P. J., T. F. Haydar, and A. E. Simon. 1993. Sequences and structures required for recombination between virus-associated RNAs. *Science* **260**:801–805.
- de Groot, R. J., R. G. van der Most, and W. J. M. Spaan. 1992. The fitness of defective interfering murine coronavirus DI-a and its derivatives is decreased by nonsense and frameshift mutations. *J. Virol.* **66**:5898–5905.
- Devereux, J., P. Haerberli, and O. Smithies. 1984. A comprehensive set of sequence analysis programs for the VAX. *Nucleic Acids Res.* **12**:387–395.
- Furuya, T., T. B. Macnaughton, N. La Monica, and M. M. C. Lai. 1993. Natural evolution of coronavirus defective-interfering RNA involves RNA recombination. *Virology* **194**:408–413.
- Hearne, P. Q., D. A. Knorr, B. I. Hillman, and T. J. Morris. 1990. The complete genome structure and synthesis of infectious RNA from clones of tomato bushy stunt virus. *Virology* **177**:141–151.
- Hillman, B. I., J. C. Carrington, and T. J. Morris. 1987. A defective interfering RNA that contains a mosaic of a plant virus genome. *Cell* **51**:427–433.
- Jarvis, T. C., and K. Kirkegaard. 1992. Poliovirus RNA recombination: mechanistic studies in the absence of selection. *EMBO J.* **11**:3135–3145.
- Jones, R. W., A. O. Jackson, and T. J. Morris. 1990. Defective-interfering RNAs and elevated temperatures inhibit replication of tomato bushy stunt virus in inoculated protoplasts. *Virology* **176**:539–545.
- Kim, Y., M. M. C. Lai, and S. Makino. 1993. Generation and selection of coronavirus defective interfering RNA with large open reading frame by RNA recombination and possible editing. *Virology* **194**:244–253.
- King, A. M. Q. 1988. Preferred sites of recombination in poliovirus RNA: an analysis of 40 intertypic cross-over sequences. *Nucleic Acids Res.* **16**:11705–11723.
- Knorr, D. A., and T. J. Morris. 1991. Origin and evolution of defective interfering RNAs of tomato bushy stunt virus, p. 57–66. *In* R. G. Herrmann and B. Larkins (ed.), *Plant molecular biology 2*. Plenum Press, New York.
- Knorr, D. A., R. H. Mullin, P. Q. Hearne, and T. J. Morris. 1991. De novo generation of defective interfering RNAs of tomato bushy stunt virus by high multiplicity passage. *Virology* **181**:193–202.
- Lai, M. M. C. 1992. RNA recombination in animal and plant viruses. *Microbiol. Rev.* **56**:61–79.
- Lazzarini, R. A., J. D. Keene, and M. Schubert. 1981. The origins of defective interfering particles of the negative-strand RNA viruses. *Cell* **26**:145–154.
- Li, X. H., L. A. Heaton, T. J. Morris, and A. E. Simon. 1989. Turnip crinkle virus defective interfering RNAs intensify viral symptoms and are generated de novo. *Proc. Natl. Acad. Sci. USA* **86**:9173–9177.
- Li, Y., and L. A. Ball. 1993. Nonhomologous RNA recombination during negative-strand synthesis of flock house virus RNA. *J. Virol.* **67**:3854–3860.
- Makino, S., N. Fujioka, and K. Fujiwara. 1985. Structure of the intracellular defective viral RNAs of defective interfering particles of mouse hepatitis virus. *J. Virol.* **54**:329–336.
- Makino, S., C.-K. Shies, L. H. Soe, S. C. Baker, and M. M. C. Lai. 1988. Primary structure and translation of a defective interfering RNA of murine coronavirus. *Virology* **166**:550–560.
- Maniatis, T., E. F. Fritsch, and J. Sambrook. 1982. *Molecular cloning: a laboratory manual*, 2nd ed. Cold Spring Harbor Laboratory Press, Cold Spring Harbor, N.Y.
- Maxam, A. M., and W. Gilbert. 1977. A new method for sequencing DNA. *Proc. Natl. Acad. Sci. USA* **74**:560–564.
- Nagy, P. D., and J. J. Bujarski. 1992. Genetic recombination in brome mosaic virus: effect of sequence and replication of RNA on accumulation of recombinants. *J. Virol.* **66**:6824–6828.
- Perrault, J. 1981. Origin and replication of defective interfering particles. *Curr. Top. Microbiol. Immunol.* **93**:151–207.
- Resende, R. D., P. de Hann, E. van de Vossen, A. C. Avila, R. Goldbach, and D. Peters. 1992. Defective interfering L RNA segments of tomato spotted wilt virus retain both virus genome termini and have extensive internal deletions. *J. Gen. Virol.* **73**:2509–2516.
- Rochon, D. M. 1991. Rapid de novo generation of defective interfering RNA by cucumber necrosis virus mutants that do not express the 20-kDa nonstructural protein. *Proc. Natl. Acad. Sci. USA* **88**:11153–11157.
- Rochon, D. M., and J. C. Johnston. 1991. Infectious transcripts from cloned cucumber necrosis virus cDNA: evidence for a bifunctional subgenomic promoter. *Virology* **181**:656–665.
- Rochon, D. M., and J. H. Tremaine. 1989. Complete nucleotide sequence of the cucumber necrosis virus genome. *Virology* **169**:251–259.
- Romero, J., Q. Huang, J. Pogany, and J. J. Bujarski. 1993. Characterization of defective interfering RNA components that increase symptom severity of broad bean mottle virus infections. *Virology* **194**:576–584.
- Roux, L., A. E. Simon, and J. J. Holland. 1991. Effects of defective interfering viruses on virus replication and pathogenesis in vitro and in vivo. *Adv. Virus Res.* **40**:181–211.

34. **Schlesinger, S.** 1988. The generation and amplification of defective interfering RNAs, p. 167–185. *In* E. Domingo, J. J. Holland, and P. Ahlquist (ed.), RNA genetics. Vol. 2. CRC Press, Inc., Boca Raton, Fla.
35. **Scholthof, H. B., T. J. Morris, and A. O. Jackson.** 1993. The capsid protein gene of tomato bushy stunt virus is dispensable for systemic movement and can be replaced for localized expression of foreign genes. *Mol. Plant-Microbe Interact.* **6**:309–322.
36. **White, K. A., J. B. Bancroft, and G. A. Mackie.** 1991. Defective RNAs of clover yellow mosaic virus encode nonstructural/coat protein fusion products. *Virology* **183**:479–486.
37. **White, K. A., J. B. Bancroft, and G. A. Mackie.** 1992. Coding capacity determines in vivo accumulation of a defective RNA of clover yellow mosaic virus. *J. Virol.* **66**:3069–3076.